Multibody Syst Dyn
https://doi.org/10.1007/s11044-018-09640-6

Modeling and analysis of friction including rolling effects in multibody dynamics: a review

Filipe Marques[1] · Paulo Flores[1] · J.C. Pimenta Claro[1] · Hamid M. Lankarani[2]

Received: 10 November 2017 / Accepted: 3 August 2018

Abstract Friction exists in most mechanical systems, and it can have a major influence on their dynamic performance and operating conditions. As a consequence of frictional contact phenomena, energy is dissipated and the state of a system can change slowly and rapidly, depending on the nature of the contact, continuous or impact condition. Other effects associated with friction in mechanical systems are the vibration and noise propagation of the system components, nonlinear systems' behavior and wear. Overall, the knowledge of the friction regimen, as well as the frictional forces developed at the interface of mechanical parts in contact with relative motion, is crucial for the dynamic analysis of mechanical systems, and has consequences in the design process. Thus, this work is a review of the modeling and analysis of frictional effects in multibody systems with the purpose of better understanding and obtaining accurate responses. In this process, pure dry sliding friction, stick–slip effect, viscous friction, Stribeck effect, and frictional lag are some of the main phenomena associated with friction, which are addressed in depth. Overall, the friction models can be divided into two main groups, namely the "static friction models" and the "dynamic friction models". The static models describe the steady-state behavior of the relation friction-force/relative-velocity, while the dynamic models allow for the capturing of more physical responses and properties by using extra state variables. In a simpler manner, the static and dynamic friction models differ mostly in the modeled frictional effects, implementation complexity, and computational efficiency. Hence, this research is aimed at analyzing in detail the role of friction modeling in the dynamic response of multibody system, as well as addressing the importance of friction models selection for accurately describing the friction related phenomena. Demonstrative application examples, which include friction in ideal mechanical joints and systems involving contact–impact events, including an example of rolling contact will be considered and investigated to illustrate the main assumptions and procedures adopted in this work. The results from this study indicate that in most cases, a static friction model, which accounts for static friction and avoids the discontinuity at zero

✉ F. Marques
fmarques@dem.uminho.pt

[1] CMEMS-UMinho, Department of Mechanical Engineering, University of Minho, Campus de Azurém, 4804-533 Guimarães, Portugal

[2] Department of Mechanical Engineering, Wichita State University, Wichita, KS 67260-133, USA

Published online: 22 August 2018

velocity, is a suitable choice. A more advanced dynamic friction model has to be developed to be utilized for systems containing high variations of normal load, namely with impact conditions.

Keywords Friction modeling · Contact forces · Multibody dynamics

1 Introduction

Historically, rolling contact study gained its relevance in a strictly mechanics of materials point of view, essentially through the characterization of the stresses and deformations arising from two solid bodies surfaces brought into contact. Railroad wheels, journal and roller bearings, gears' teeth, and cylinder seals were the most studied mechanical components, where design for efficiency and reliability has been the main focus. Later, the concepts of "conformal" and "non-conformal" contacts were developed, leading to the "surface" and the "point/line" contact approaches, with a special highlight on the latter. In this concept, highly concentrated pressures lead to relevant local deformations, thus influencing the real shape of the contact itself. It has been stated that the study of contact mechanics increases its complexity considerably due to the influence of the relative motion of the contacting surfaces. An example is the meshing of a pair of gear teeth where rolling and sliding occurs simultaneously. These phenomena have been extensively addressed in the literature [1–3].

From Hertz works on smooth, elastic and frictionless contacts [4], using simple Coulomb dry friction laws [5], and taking into consideration the concentric radial stress distribution due to concentrated forces, as characterized by Flamant [6], and Timoshenko's equations of elasticity [7], quasi-static and kinetics approaches have been developed. These methodologies consist of the coupling of normal and tangential contact forces, which can capture phenomena such as perfect non-slip and/or sliding rolling motion. Furthermore, the introduction of plasticity and viscoelasticity behaviors [8, 9], contact elastohydrodynamics [10], as well as material hardening, and fatigue phenomena [11–13], fostered materials mechanics design of rolling contacts to a higher level of reliability [14–16].

Simultaneously, the tribological approach on the contact dynamics focused on the surface topography issues, highlighting the role of roughness micro-surfaces and "point" contacts interaction of asperities, i.e., materials hardness dissimilarity, elastic or plastic deformation, local hardening effects, micro-welding, and picks rupture. These phenomena lead to different wear mechanisms, such as adhesion and abrasion, but also fretting, stretching, fatigue, brittle fracture, tribochemical reaction and erosion phenomena. They differ depending on the pair of mating materials, on the working conditions, as well as on the environmental variables. Several semi-empirical and theoretical wear models had been developed, such as the "Johnson–Kendall–Roberts" [17] and "Derjaguin–Muller–Toporov" [18], among others. Similarly, a wide range of friction modeling mechanisms had been proposed [19–23], which became quite popular with the advent of computational methods. Nevertheless, even previously to these in due time widely used approaches, other models were developed, namely addressing nonlinear friction–load dependency and the asperities/real contact area importance [24], stress/strain proportional laws [25], and considerations between picks elastic deformation and/or brittle rupture [26]. It must be noted that although these methodologies focused on dry adhesion conditions in several aspects, they were contradicting each other, and also the traditionally accepted Coulomb's law. Subsequently, more elaborated models coupled adhesion with abrasion and deformation, showing the influence of sliding distance

on friction coefficient [27], incorporating traditional plasticity theory [28], the effect of debris (the "3rd body" theory) interfaces [29], or the prediction of elastic growth of real contact area during adhesion [30]. A more extensive analysis on these and other improved friction models, for inclusion in analytical or numerical methods, can be found in [31].

Modeling dry contact between mating surfaces with relative motion can induce severe instabilities [32, 33], independently of the utilized friction model. Thus, these instabilities might be produced due to dynamic changes in kinematic conditions of the multibody system, which inevitably occurs, for instance, in most revolute hinges or linear guides, even when operating under steady state conditions. However, these instabilities can also arise from running in abnormal conditions, namely thermal expansion due to friction, variation of friction force with sliding speed, change in contact/wear mechanisms due to variations of speed or transmitted load, or may be generated by pure dynamic effects of the friction process by itself [34, 35]. The latter relates with the well-known "stick–slip" phenomenon [36–38], which can be physically explained by the strong surface bounding/adhesion or micro-welding between asperity picks when the relative tangential velocity is low, leading to an extremely nonlinear behavior with high frequency. From the dynamical point of view, the friction force tends to increase at low relative velocities, which causes the surfaces to stick. In order to return to the sliding state, the external tangential force applied must exceed the static friction force, and, therefore break the adhesion bounds. Other features are also quite relevant when modeling the elastohydrodynamics effects [39–41], although it is not in the scope of this work.

In the context of multibody systems dynamics, several friction force models can be utilized to evaluate the tangential forces generated during the contact [22, 23]. The selection of the friction force model depends on several factors [23], such as the complexity of the problem to be solved, the computational efficiency, the capability to characterize the contacting surfaces, the necessity of capturing different phenomena, among others. These models are mainly divided between "static" and "dynamic" friction models. The former only describes the steady-state relation between friction force and relative velocity. In turn, the dynamic models may capture more frictional characteristics due to the inclusion of extra-state variables. Despite the fact that the more basic and simpler models can only take into account kinetic friction, by increasing their complexity and scope, they may consider other aspects such as static friction, Stribeck effect, pre-sliding displacement, or frictional lag. Typically, the more advanced models require more parameters to be completely defined and implemented. This may become a significant issue, mainly if some of the parameters are not directly related with the physical properties of the contacting surfaces, and therefore more challenging problem to be resolved. Several authors have proposed numerical and experimental methodologies for the identification of friction models' parameters [42–45]. Most of these approaches have been developed with the focus on the dynamic models, since they present parameters which are more difficult to be estimated, such as the stiffness and damping of the bristles. Within the dynamic friction force models, LuGre model [47] appears to be the most well-accepted in the literature due to its wide utilization [42, 44, 46, 48]. Furthermore, some researchers have proposed a few modifications to the LuGre model to improve its performance on certain conditions, namely a specific application [46], a specific phenomenon [49], or under variation of normal load [50]. This indicates that a general friction force model capable of addressing a variety of different problems and capturing different phenomena is basically not available.

The main objective of this work is to provide some insights on the modeling of friction forces in a multibody dynamics simulation, with a special focus on rolling scenarios, as it is demonstrated by the provided application examples. The structure of the paper is organized

as follows. Section 2 presents a succinct description of the most used approaches for the evaluation of frictional forces, from the simplest to the most complex. Section 3 provides a general description of multibody dynamics formulation using the Newton–Euler equations and including frictional effects. Two application examples are used to examine and discuss the most important issues in modeling friction on dynamic simulation. The first example is a planar roller–crank mechanism with continuous frictional contact between the roller and the ground. In turn, the second application example involves friction modeling during impact events, considering a journal–bearing system for that purpose. Finally, the summary and main conclusions of this work are stated in Sect. 6.

2 Friction force models

This section provides a brief overview of the most frequently used methodologies to model tangential contact forces in the context of multibody dynamics. As previously mentioned, most of the contact interactions between different bodies can be modeled as point or line contact, where the contact patch is reduced to a single point (or line). Therefore, the normal pressure and tangential traction distributions are neglected, and simplified to force loads, which comprehensively diminishes the computational cost and is a quite suitable approximation, when studying the dynamics of a mechanical multibody system. For a detailed analysis, such as wear or contact fatigue predictions, contact shape and size, as well as stress distributions must be considered [51], which are not within the scope of this work.

Most of the authors typically divide the friction force models in two main groups, the "static" and "dynamic" models [22, 23]. The static models only describe the steady-state behavior of friction force–relative velocity relation, which makes them easy to implement in a multibody dynamics code.

The first developed friction model dates back to 1785, when Coulomb [5] stated that friction force always opposes to the relative motion between two contacting surfaces, and its magnitude is proportional to the normal contact force. This model can be mathematically described as follows:

$$\mathbf{F}_{\mathrm{F}} = \begin{cases} F_{\mathrm{C}}\,\mathrm{sgn}(\mathbf{v}_{\mathrm{T}}) & \text{if } \|\mathbf{v}_{\mathrm{T}}\| \neq 0 \\ \min(\|\mathbf{F}_{\mathrm{e}}\|, F_{\mathrm{C}})\,\mathrm{sgn}(\mathbf{F}_{\mathrm{e}}) & \text{if } \|\mathbf{v}_{\mathrm{T}}\| = 0, \end{cases} \tag{1}$$

where

$$F_{\mathrm{C}} = \mu_{\mathrm{k}} \|\mathbf{F}_{\mathrm{N}}\|, \tag{2}$$

in which $\mathbf{F}_{\mathrm{N}}$ is the normal contact force, μ_{k} denotes the kinetic coefficient of friction, F_{C} represents the magnitude of Coulomb friction, $\mathbf{F}_{\mathrm{e}}$ is the external tangential force, and $\mathbf{v}_{\mathrm{T}}$ denotes the relative tangential velocity of the contacting surfaces. Although the friction force does not depend on the magnitude of the relative velocity, as shown in Fig. 1a, it varies with its direction, which is defined by the *signum* function,

$$\mathrm{sgn}(\mathbf{v}_{\mathrm{T}}) = \begin{cases} \frac{\mathbf{v}_{\mathrm{T}}}{\|\mathbf{v}_{\mathrm{T}}\|} & \text{if } \|\mathbf{v}_{\mathrm{T}}\| \neq 0 \\ \mathbf{0} & \text{if } \|\mathbf{v}_{\mathrm{T}}\| = 0, \end{cases} \tag{3}$$

where $\mathbf{0}$ is a null vector of the same dimension as $\mathbf{v}_{\mathrm{T}}$.

Coulomb's law is the simplest and most utilized friction force model, since it only requires one input parameter, i.e., the kinetic coefficient of friction, and it is a suitable choice for most of the dynamical systems where friction does not play a main role. However, it

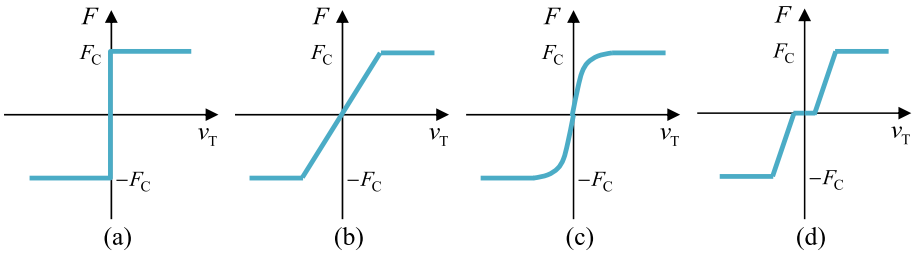

Fig. 1 Representation of (**a**) the classical Coulomb friction model and (**b–d**) alternative approaches to avoid the discontinuity at zero velocity

presents several numerical problems due to the existent discontinuity at zero relative tangential velocity. To avoid numerical instability, several authors proposed different approaches to deal with the friction discontinuity [52–54], which consists of replacing the original function by a smoother one in the neighborhood of zero velocity. Typically, these approaches use extra tolerance parameters to define the degree of smoothness. Some of these alternatives are depicted in Figs. 1b–d.

Although Coulomb's law presents a suitable approximation, it is well established that the magnitude of friction force varies with the relative velocity. Indeed, friction at zero velocity, i.e., static friction, is higher than kinetic friction, and it decreases continuously with the increase of relative velocity. This is the so-called Stribeck effect. Several expressions can be found for modeling this phenomenon [55–59], of which the following is the most utilized in the literature:

$$\mathbf{F}_F = \left(F_C + (F_S - F_C)e^{-(\frac{\|\mathbf{v}_T\|}{v_S})^{\delta_\sigma}}\right)\mathrm{sgn}(\mathbf{v}_T) + F_v\mathbf{v}_T, \tag{4}$$

where

$$F_S = \mu_s\|\mathbf{F}_N\|, \tag{5}$$

in which μ_s denotes the static coefficient of friction, F_S is the magnitude of static friction, v_S represents the Stribeck velocity, δ_σ is an exponent which relies on the geometry of the contacting surfaces, often considered to be equal to 2, and F_v is the viscous friction coefficient. In lubricated contacts, it is usual to adopt a linear relationship between the relative velocity and friction force, the value of viscous coefficient relates to the lubricant's viscosity. However, in this work, only dry contact is addressed, which involves neglecting the viscous friction coefficient. Thus, Fig. 2a shows the shape for the Stribeck curve, which also contains a discontinuity at zero relative tangential velocity. As in the case of Coulomb's friction law, this discontinuity creates several numerical issues during a dynamic simulation. Therefore, several researchers have proposed different approaches to prevent numerical instability [54, 60, 61], two of these alternatives can be seen in Figs. 2b–c.

Recently, Brown and McPhee [61] proposed a new friction model, which is suitable to be applied in real-time simulations and optimization problems, since it is continuously differentiable and only velocity-dependent. Neglecting the viscous friction term, it can be expressed as

$$\mathbf{F}_F = \left(F_C\tanh\left(4\frac{\|\mathbf{v}_T\|}{v_S}\right) + (F_S - F_C)\frac{\frac{\|\mathbf{v}_T\|}{v_S}}{(\frac{1}{4}(\frac{\|\mathbf{v}_T\|}{v_S})^2 + \frac{3}{4})^2}\right)\mathrm{sgn}(\mathbf{v}_T). \tag{6}$$

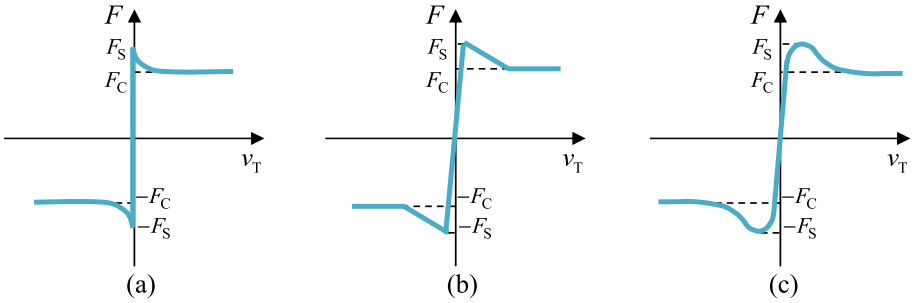

Fig. 2 Representation of (**a**) the classical Stribeck curve and (**b–c**) alternative approaches to avoid the discontinuity at zero velocity

This model is a suitable alternative to the classical Stribeck curve, since it avoids the discontinuity and requires the same number of parameters. Its friction–velocity dependence resembles the shape depicted in Fig. 2c.

Due to the importance of friction forces on the dynamic behavior of most mechanical systems, many researchers found that the static friction force models are not able to capture several phenomena associated with frictional interaction, such as pre-sliding displacement or frictional lag [62, 63]. Therefore, this need led to the development of more advanced friction models, which used extra state variables for modeling the evolution of friction forces. These models are known as dynamic models since they evaluate the friction forces not only based on the actual state of the contact, but also based on the contact history.

Generally, the dynamic friction models use an extra state variable $\mathbf{z}$, which is the average of bristle deflection that represents the behavior of surface asperities during contact interaction. The bristles may behave as springs during the sticking phase.

The Dahl friction model [64, 65] was the first dynamic model to be developed with the aim of describing the friction behavior of ball bearings. Although, this model does not include static friction, it allows the friction force to vary, being proportional to the average bristle deflection as

$$\mathbf{F}_F = \sigma_0 \mathbf{z}, \tag{7}$$

where σ_0 is the stiffness of the bristles, and the behavior of $\mathbf{z}$ is modeled by the following differential equation:

$$\frac{d\mathbf{z}}{dt} = \left(1 - \frac{\sigma_0}{F_C}\mathbf{z} \cdot \mathrm{sgn}(\mathbf{v}_T)\right)\mathbf{v}_T. \tag{8}$$

This new state variable allows for the capture of the pre-sliding displacement, which eliminates the discontinuity at zero velocity.

Since Dahl's model [64], many researchers have proposed other dynamic friction models, which can describe additional friction phenomena. Indeed, the LuGre model [47] appears to be the most accepted in the scientific community being the most widely used. This model can also capture the Stribeck and stiction effects, as well as frictional lag and pre-sliding displacement. These phenomena represent the dynamic characteristics of frictional effects. Thus, the pre-sliding displacement is characterized by a small motion in the elastic range when the applied force is less than the break-away force, and the frictional lag is the delay in the change of friction force as a function of velocity.

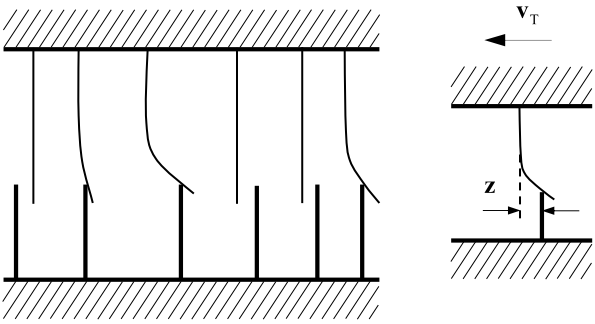

Fig. 3 Physical interpretation of dynamic friction models and average bristle deflection

To quantify the average bristle deflection, it is necessary to introduce an internal state variable $\mathbf{z}$, as it is represented in Fig. 3. Thus, the LuGre model follows as

$$\frac{d\mathbf{z}}{dt} = \left(1 - \frac{\sigma_0}{G(\mathbf{v}_T)}\mathbf{z} \cdot \text{sgn}(\mathbf{v}_T)\right)\mathbf{v}_T, \tag{9}$$

$$\mathbf{F}_F = \sigma_0\mathbf{z} + \sigma_1\frac{d\mathbf{z}}{dt} + \sigma_2\mathbf{v}_T, \tag{10}$$

where σ_1 is the damping of the bristles, σ_2 denotes the viscous friction coefficient, is an arbitrary function that describes the viscous effect, and $G(\mathbf{v}_T)$ is an arbitrary function, which describes the Stribeck curve and can be defined by

$$G(\mathbf{v}_T) = F_C + (F_S - F_C)e^{-(\frac{\|\mathbf{v}_T\|}{v_S})^{\delta\sigma}}. \tag{11}$$

Furthermore, the Generalized Maxwell Slip model [66, 67] is an enhanced methodology which represents the pre-sliding hysteresis, and considers several parallel frictional connections. This model has been becoming popular in the control community.

Although the dynamic models can consider more characteristics of frictional behavior, they have a high computational cost since they demand a reduction of the integration time step due to making the problem numerically stiffer. For more detailed information on this topic, the interested reader may see some fundamental literature [22, 23].

3 Multibody dynamics formulation with friction

A general multibody system can be defined as a set of bodies, which are interconnected by kinematic joints and undergone to the action of generalized force elements. The joints not only connect the different bodies, but also constrain their relative motion in several forms by eliminating some of their relative degrees of freedom. For a constrained multibody system, the kinematic joints can be characterized by a set of algebraic equations in the following form [68]:

$$\boldsymbol{\Phi}(\mathbf{q}, t) = \mathbf{0}, \tag{12}$$

where $\mathbf{q}$ denotes the vector of generalized coordinates and t is the time variable. Each kinematic or ideal joint contributes with a different number of equations depending on the number of degrees of freedom it constrains. The velocity constraint equations can be obtained

by differentiating Eq. (12) with respect to time. After a second differentiation with respect to time, the acceleration constraint equations are obtained as

$$\boldsymbol{\Phi}_{\mathbf{q}}\ddot{\mathbf{q}} = \boldsymbol{\gamma}, \tag{13}$$

in which $\boldsymbol{\Phi}_{\mathbf{q}}$ denotes the Jacobian matrix of the constraint equations, $\ddot{\mathbf{q}}$ is the vector of generalized accelerations, and $\boldsymbol{\gamma}$ represents the right-hand side of the acceleration equations, which contains the terms that are exclusively function of velocity square terms.

Regarding the dynamics of a system of rigid bodies, the Newton–Euler formulation can be used to express the translation and rotational equations of motion in the following form:

$$\mathbf{M}\ddot{\mathbf{q}} = \mathbf{g}, \tag{14}$$

where $\mathbf{M}$ denotes the global mass matrix of the system, containing the mass and moments of inertia, and $\mathbf{g}$ is the vector of generalized forces that contains all the external forces and moments acting on the multibody system.

In order to derive the equations of motion for a constrained multibody system, Eq. (14) can be expanded using the Lagrange multipliers technique that includes the reaction forces in the joints, which are given by

$$\mathbf{g}^{(\mathbf{c})} = -\boldsymbol{\Phi}_{\mathbf{q}}^{T}\lambda, \tag{15}$$

where $\boldsymbol{\lambda}$ represents the vector of the Lagrange multipliers. Adding Eq. (14) to the acceleration constraint equations (13), the equation of motion of a general constrained multibody system can be written as [68]

$$\begin{bmatrix} \mathbf{M} & \boldsymbol{\Phi}_{\mathbf{q}}^{T} \\ \boldsymbol{\Phi}_{\mathbf{q}} & \mathbf{0} \end{bmatrix} \begin{Bmatrix} \ddot{\mathbf{q}} \\ \boldsymbol{\lambda} \end{Bmatrix} = \begin{Bmatrix} \mathbf{g} \\ \boldsymbol{\gamma} \end{Bmatrix}. \tag{16}$$

This system of equations must be solved to obtain the generalized accelerations, which are integrated over time. However, for long duration simulations, the constraint equations tend to be violated due to errors introduced by the numerical integration process and by the inaccuracy of the initial conditions. In order to handle the constraint violation, several approaches can be adopted, i.e., constraint stabilization techniques, coordinate partitioning methods, and direct correct formulations [69]. In this work, the Baumgarte stabilization technique is applied, and Eq. (16) is modified to

$$\begin{bmatrix} \mathbf{M} & \boldsymbol{\Phi}_{\mathbf{q}}^{T} \\ \boldsymbol{\Phi}_{\mathbf{q}} & \mathbf{0} \end{bmatrix} \begin{Bmatrix} \ddot{\mathbf{q}} \\ \boldsymbol{\lambda} \end{Bmatrix} = \begin{Bmatrix} \mathbf{g} \\ \boldsymbol{\gamma} - 2\alpha\dot{\boldsymbol{\Phi}} - \beta^{2}\boldsymbol{\Phi} \end{Bmatrix}, \tag{17}$$

where α and β are positive constants that represent the feedback control parameters for the velocity and position constraint violations [70, 71]. For each time step, Eqs. (17) must be solved in order to the accelerations, and together with the system's velocities, are integrated to obtain the positions and velocities of the following time step.

The inclusion of friction in multibody system dynamic simulation can be a cumbersome task due to its nonlinear nature and numerical difficulties associated with it. There are different ways of including friction into the equations of motion depending on the type of contact problem to be solved. As it was previously discussed in Sect. 2, the friction force strongly depends on the normal contact force, therefore the first step in friction implementation is to analyze its origin. For contact cases where the interaction forces are treated as external forces (i.e., impact simulation using penetration approach), both normal and friction forces are simply included in the vector of forces $\mathbf{g}$, and calculated independently in each time step. However, when the normal contact force is calculated implicitly during the resolution of the equations of motion (i.e., the reaction forces in the kinematic joints), a different methodol-

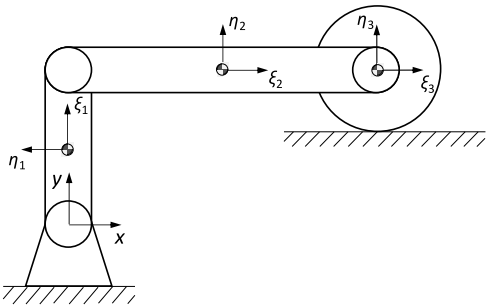

Fig. 4 Representation of the initial configuration of planar roller–crank mechanism

ogy must be considered since the normal load is not known when the system of equations is constructed. Several researchers [23, 72–79] experienced this issue, which led to the development of several approaches to handle this problem. Haug [76] proposed using a space tangent formulation to solve the equation of motion with friction. Additionally, Harlecki and Urbas [78] used a Newmark iterative algorithm to solve the equations of motions of one degree of freedom mechanisms with frictional joints. Frączek and Wojtyra [75] also utilized an iterative procedure to find the corrected reaction forces to apply in friction calculation.

For some of the existent formulations, considering Coulomb's friction law with discontinuity at zero velocity may create problems of nonuniqueness of the solution [75, 77, 80, 81]. Moreover, the modeling of friction recurring to dynamic models presents an additional issue, which is related to the use of extra-state variables to describe the friction force. These state variables must be integrated over time, while solving the differential equations associated with each dynamic friction model. Two approaches can be employed. In the first approach, the frictional state variables can be added to the remaining state variables (generalized coordinates and velocities) and integrated with them. In the second approach, these variables can be integrated locally during the resolution of friction problem. Although both options are acceptable, the most suitable choice may differ depending on the integration algorithm being utilized, or the type of contact problem. Furthermore, the use of these models typically increases the numerical stiffness of the problem, which may slow down the simulation.

4 Application example 1: 2D roller–crank mechanism

In this section, a planar roller–crank mechanism is employed as first application example to examine the issues associated with modeling friction on continuous contact problems. Figure 4 shows a representation of the roller–crank mechanism and its initial configuration. The mechanism is constituted by three different bodies, namely the crank, the connecting rod and the roller. The geometrical and inertial properties of the bodies are listed in Table 1. The system is constituted by three perfect revolute joints (ground–crank; crank–rod; rod–roller), and the movement of the roller is also constrained in the y-direction. Therefore, this mechanical system has two degrees-of-freedom, the first is associated with the overall motion of the mechanism constituted by the loop, and the second is related with the rotational movement of the roller. The initial angular velocity of the crank was defined as 4 rad/s in the anticlockwise direction, and the remaining velocities were determined such as the kinematic constraints were fulfilled and the roller starts the simulation in a pure rolling state, i.e., with no slip. The initial conditions of the system are listed in Table 2. In this example, the friction modeling is only included in the contact interaction between the roller and the ground, therefore, the frictional forces will affect not only the energy dissipation of the sys-

Table 1 Geometrical and inertial properties of each body

Body	Length/radius [m]	Mass [kg]	Moment of inertia [kg m^2]
Crank	0.10	0.12	0.002
Rod	0.30	0.30	0.002
Roller	0.05	0.10	0.001

Table 2 Initial positions and velocities of each body

Body	Position			Velocity		
	x [m]	y [m]	θ [rad]	v_x [m/s]	v_y [m/s]	ω [rad/s]
Crank	0.00	0.05	$\pi/2$	-0.2	0.0	4.0
Rod	0.15	0.10	0.00	-0.4	0.0	0.0
Roller	0.30	0.10	0.00	-0.4	0.0	8.0

Table 3 Parameters considered for the different friction models

Parameter	Symbol	Value
Static coefficient of friction	μ_s	0.15
Kinetic coefficient of friction	μ_k	0.1
Stribeck velocity	v_s	0.001 m/s
Geometry factor	δ_σ	2
Stiffness coefficient	σ_0	10^5 N/m
Damping coefficient	σ_1	$\sqrt{10^5}$ Ns/m
Coefficient of viscosity	σ_2	0 Ns/m

tem, but also the state of their relative motion (pure rolling, partial slip, or pure slip). Since the vertical movement between the roller and the ground is kinematically constrained, the normal force in the contact surface is obtained as a constraint reaction. Beyond the reaction, inertia and friction forces, only gravitational forces are considered, which are applied in the negative direction of y axis as external forces.

In order to perform a comparative study between different friction models, the tangential force in the contact between the roller and the ground was computed recurring to six different methodologies, namely discontinuous Coulomb, regularized Coulomb, discontinuous Stribeck curve, Brown and McPhee model, Dahl's model, and LuGre model. The parameters used for the referred friction force models are listed in Table 3, and they were selected based on typical values found on the literature.

The numerical simulations were performed for two seconds of mechanism's motion, and the results were compared through the analysis of the angular acceleration of the roller, which has directly affected by the tangential force in the contact. Figure 5 shows that the main differences between the results from the different models are in the first part of the motion since the roller starts with null relative tangential velocity in the contact, therefore in a sticking phase. The discontinuous Coulomb and Stribeck friction models demonstrate high numerical instability during the initial phase due to their discontinuity for zero velocity. It should be noted that it is not possible to simulate the mechanism motion with these two friction models using a variable time step algorithm, since the algorithm is not able to proceed when it deals with the discontinuous behavior. Another significant difference

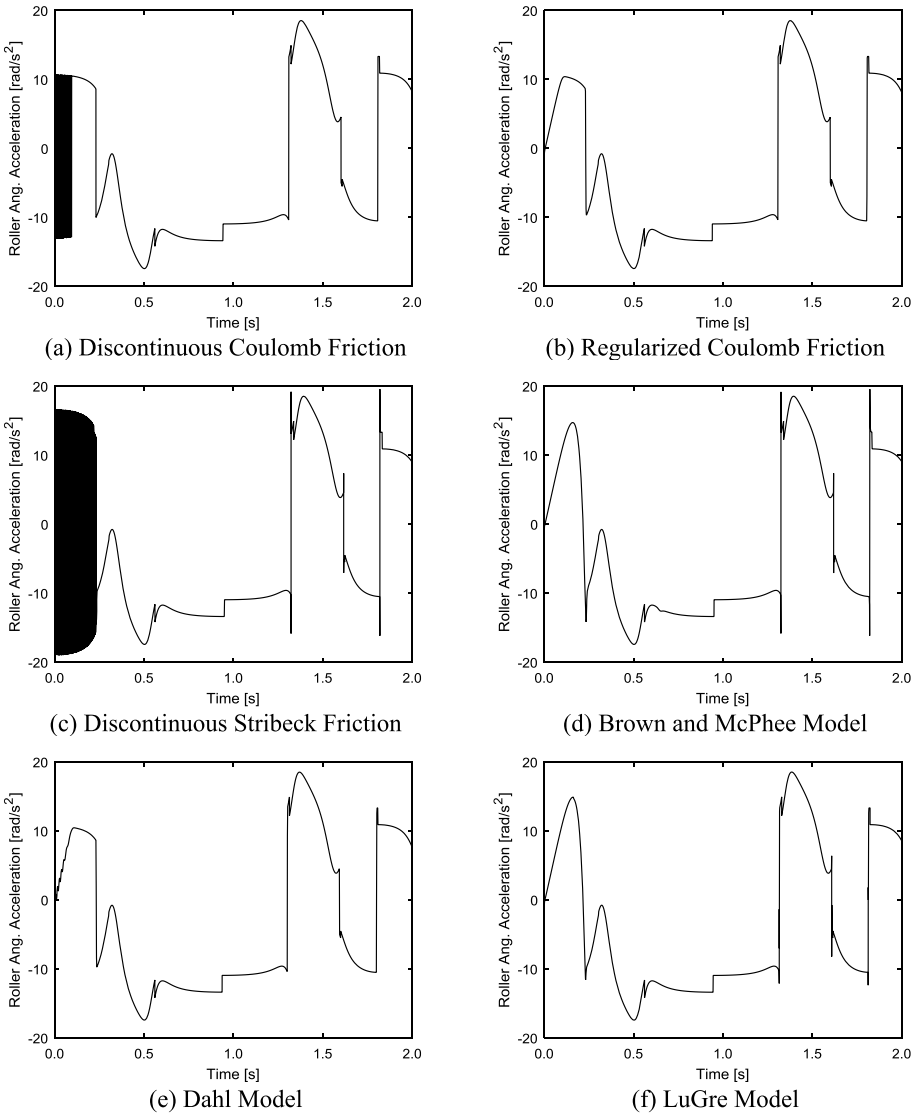

Fig. 5 Comparison of roller's angular acceleration for different friction models

between the presented results subsist on that the models which do not consider static friction (discontinuous Coulomb, regularized Coulomb, and Dahl). These cannot maintain the sticking behavior until for higher accelerations, when compared with the remaining models (discontinuous Stribeck, Brown and McPhee, and LuGre). The Brown and McPhee and LuGre models seem to be more appropriate since they do not present unstable behavior and can take into account the static friction. As shown in Fig. 5, they produce a similar angular acceleration, with some differences on the acceleration peaks when the relative velocity passes through zero. Comparing the relative tangential velocity on the contact point for both models during the first 0.2 seconds of simulation where stiction occurs (see Fig. 6), it can be observed that the Brown and McPhee model allows having a major drift on the relative

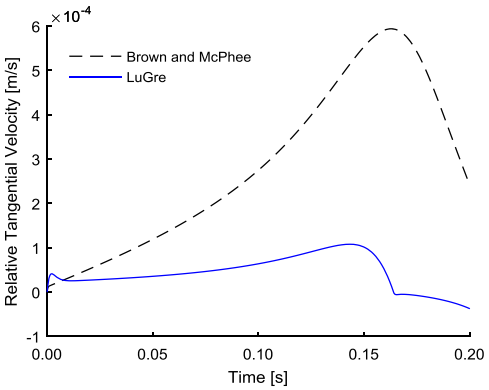

Fig. 6 Comparison of relative tangential velocity for the sticking phase

tangential velocity since it does not depend on the relative displacement. As a dynamical model, the LuGre model accounts for the pre-sliding displacement, this allows not having the same artificial slip.

For a more detailed comparison, the ratio between friction and normal force during the entire simulation was analyzed. Figure 7 presents this ratio as a function of the relative tangential velocity. As expected, for the static friction models, which cannot describe a transient behavior, this ratio is constant for a specific tangential velocity. Actually, the curves in Figs. 7a–d match with their description as described in Sect. 2. In turn, the dynamic models, namely Dahl and LuGre, present different friction–velocity relationship. Analyzing in detail from Fig. 7f, it is possible to see that LuGre model does not show the expected behavior since the ratio between friction and normal forces exceeds 0.15, which is the value for the static friction coefficient. Moreover, this ratio also shows abnormal variations near zero relative velocity. These phenomena can be explained through the examination of Eqs. (9) and (10), which describe the friction model, where two main aspects must be highlighted. Firstly, the second term in Eq. (10), which represents the bristle damping, does not depend on the normal load. Thus, the selection of bristle damping must depend on the normal load; otherwise, for different normal loads, LuGre model will produce the same magnitude of damping force which will affect differently the dynamic response. Secondly, according to Eq. (9), the LuGre model tends to meet the Stribeck curve in steady-state (constant relative tangential velocity); however, variations of normal load can greatly affect the variation of bristle deflection which does not reproduce the expected behavior. Wojtyra addressed this issue in his examination of the LuGre model [50]. Figure 8 shows the normal force in the contact during the simulation with the LuGre model, and is evident that it changes significantly. Therefore, it may not be possible to fully trust on the results with the LuGre model without constant normal force. However, for constant load cases, this model presents acceptable results [20]. Regarding the computational efficiency of the presented friction force models, Table 4 displays the relative computational time of the simulations of the roller–crank mechanism, as well as the specified options for the MATLAB solver *ode45*. The fastest models are the regularized Coulomb and Brown and McPhee, while the discontinuous ones are significantly slower due to their numerical problems. Moreover, the stiffness introduced by the extra-state variables makes the dynamic friction models the least efficient solution.

5 Application example 2: journal–bearing system

The second application example presented in this work relies on a simple journal–bearing system with clearance, as depicted in Fig. 9 [82, 83]. Since the bearing and journal are

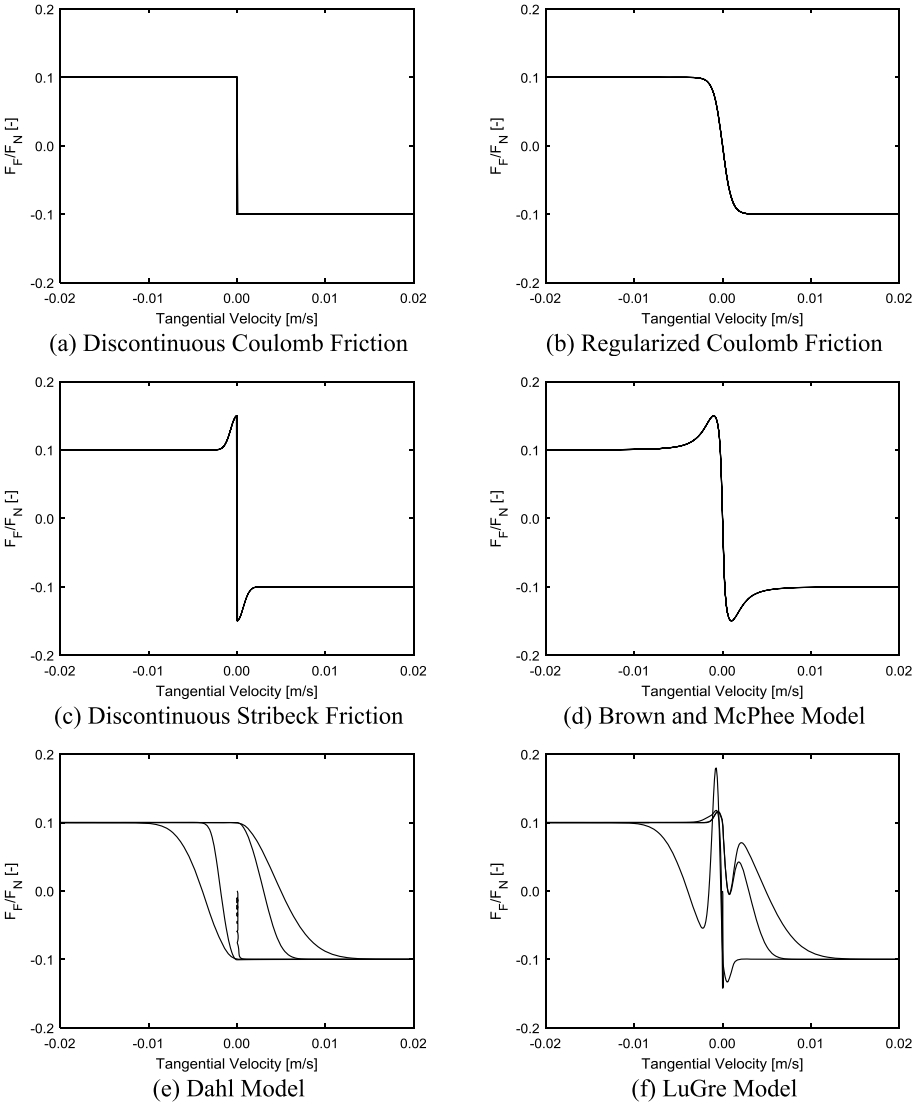

Fig. 7 Comparison of ratio between both friction and normal forces for different friction models

treated as colliding bodies, this example allows us to examine the influence of using different friction models under impact conditions where the normal loads variations are quite significant. The radial clearance allows the relative motion of the two bodies and can be defined as the difference between their radii as

$$c_{\mathrm{r}} = R_{\mathrm{B}} - R_{\mathrm{J}}, \tag{18}$$

where R_{B} and R_{J} are the radii of the bearing and journal, respectively.

Figure 10 shows two bodies i and j, respectively, the bearing and journal, and points O_i and O_j define their centers of mass which are coincident with center of the elements. Thus,

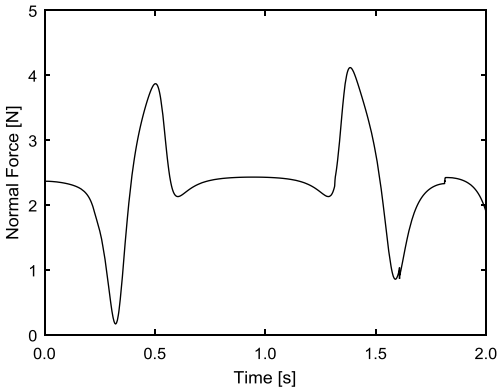

Fig. 8 Normal contact force for LuGre model

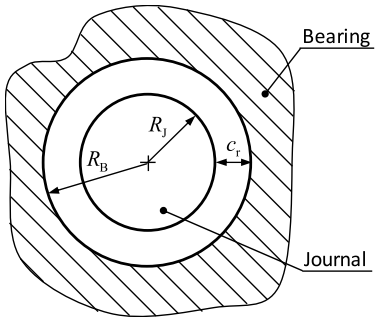

Fig. 9 Representation of a journal–bearing system

Table 4 Parameters for the time integration scheme and the relative computational time

Parameter	Value
RelTol	1e-6
AbsTol	1e-6
Friction model	**Relative computational time**
Discontinuous Coulomb friction	10.2
Regularized Coulomb friction	1
Discontinuous Stribeck friction	26.4
Brown and McPhee model	1.1
Dahl model	169.8
LuGre model	165.5

the eccentricity vector which connects the center of bearing and journal can be expressed as

$$\mathbf{e} = \mathbf{r}_j - \mathbf{r}_i, \tag{19}$$

where $\mathbf{r}_i$ and $\mathbf{r}_j$ are, respectively, the coordinates of the centers of journal and bearing in absolute coordinates.

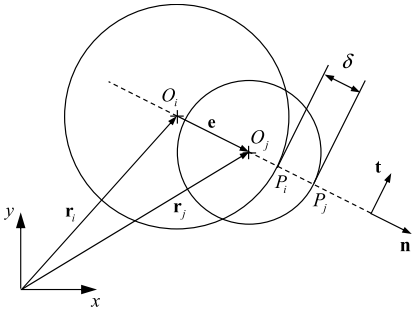

Fig. 10 General journal–bearing system with penetration

Hence, the unit normal vector to the contact plane can be given as

$$\mathbf{n} = \frac{\mathbf{e}}{e}, \tag{20}$$

where e is the magnitude of eccentric vector that is defined as

$$e = \sqrt{\mathbf{e}^T \mathbf{e}}, \tag{21}$$

In this approach, although the bodies are considered to be rigid, they are allowed to interpenetrate during contact motion. Therefore, the penetration depth is calculated as follows:

$$\delta = e - c_{\mathrm{r}}. \tag{22}$$

In turn, the velocity on the contact point can be decomposed in the normal and tangential direction to the contact. The normal velocity, or penetration velocity, establishes whether the bodies are approaching or separating, and is expressed as

$$\dot{\delta} = \left(\dot{\mathbf{r}}_j^P - \dot{\mathbf{r}}_i^P\right)^T \mathbf{n}, \tag{23}$$

where $\dot{\mathbf{r}}_i^P$ and $\dot{\mathbf{r}}_j^P$ are the global velocities of the contacting points P_i and P_j, respectively, and can be computed by the following expression:

$$\dot{\mathbf{r}}_k^P = \dot{\mathbf{r}}_k + \omega_k R_k \mathbf{t} \quad (k = i, j), \tag{24}$$

in which ω_k denotes the angular velocity of body k, and $\mathbf{t}$ is a tangent unit vector to the contact plane that is obtained by rotating vector $\mathbf{n}$ by 90° anticlockwise. Accordingly, the tangential velocity vector is calculated as

$$\mathbf{v}_{\mathrm{T}} = \left[\left(\dot{\mathbf{r}}_j^P - \dot{\mathbf{r}}_i^P\right)^T \mathbf{t}\right]\mathbf{t}. \tag{25}$$

The normal and tangential contact forces act on the defined contact points with the same direction as vectors $\mathbf{n}$ and $\mathbf{t}$, respectively. Moreover, for the normal force, a model based on Hertzian theory, together with a dissipation term, is considered here. Thus, the Lankarani–Nikravesh model [84] is utilized to calculate the normal contact load as

$$F_{\mathrm{N}} = K\delta^n \left[1 + \frac{3(1 - c_{\mathrm{e}}^2)}{4} \frac{\dot{\delta}}{\dot{\delta}^{(-)}}\right], \tag{26}$$

where c_e represents the coefficient of restitution, n is an exponent that defines the nonlinearity of the contact, which is set 1.5 for metallic contacts, $\dot{\delta}^{(-)}$ represents the initial impact velocity, and K denotes the contact stiffness that is calculated as

$$K = \frac{4}{3(\sigma_i + \sigma_j)} \left(\frac{R_i R_j}{R_i - R_j} \right)^{1/2}, \tag{27}$$

in which

$$\sigma_k = \frac{1 - \nu_k^2}{E_k} \quad (k = i, j), \tag{28}$$

where E and σ represent the Young's modulus and the Poisson ratio of the contacting materials.

Regarding the frictional forces, they are computed following the methodologies presented in Sect. 2. To compare the utilization of a static and a dynamic friction force model accounting with static friction, only the Brown and McPhee [61] and the LuGre [47] models are utilized here. The parameters for the friction force models are the same as in the previous example, which are listed in Table 3.

As it was stated in the previous example, the LuGre model presents some numerical issues in the presence of normal force variations. Thus, for this example, where impact motion exists, the stated issues gain significant importance. Therefore, the journal–bearing motion is simulated recurring to two different versions of LuGre model, namely the classical version presented in Sect. 2, and a modified version proposed by Wojtyra [50], in which Eqs. (9) and (10) are replaced by

$$\frac{d\mathbf{z}}{dt} = \left(1 - \frac{\sigma_0}{N_E g(\mathbf{v}_T)} \mathbf{z} \cdot \mathrm{sgn}(\mathbf{v}_T) \right) \mathbf{v}_T, \tag{29}$$

$$\mathbf{F} = \left(\frac{\sigma_0}{N_E} \mathbf{z} + \frac{\sigma_1}{N_E} \frac{d\mathbf{z}}{dt} \right) \|\mathbf{F}_N\|, \tag{30}$$

where the viscous friction is neglected, N_E denotes a constant equivalent normal load, and $g(\mathbf{v}_T)$ can be related to the Stribeck curve being multiplied by the normal force, as

$$G(\mathbf{v}_T) = g(\mathbf{v}_T) \|\mathbf{F}_N\|. \tag{31}$$

In this example, the equivalent normal load was considered to be equal to the weight of the journal, since it represents the normal load which guarantees the static equilibrium of the system. For this analysis, it is also considered that the bearing is attached to a fixed reference frame. The initial conditions are defined such as the journal and bearing are concentric, and the journal is rotating at 2π rad/s clockwise. The journal's motion is the result from the forward dynamic simulations which are performed with only gravitational forces and without any driver constraint. The remaining properties for the simulations are listed in Table 5, and the simulations were performed for 2 seconds of the system's motion. Moreover, the clearance size utilized here is within the clearance fits established in ISO 286 [85]. It should be noted that the inclusion of an entire mechanical system instead of a simple journal–bearing system would greatly affect the inertia of the system and, therefore, its dynamic response.

The results from the different simulations are analyzed through the motion of the journal. Figure 11 shows the eccentricity of the journal (dotted line) inside the clearance circle (solid line). In these plots, three types of motion can be identified: (i) free flight (when the

Table 5 Parameters for the dynamic simulation with the revolute clearance joint

Parameter	Value	Parameter	Value
Radius of bearing, R_i	10 mm	Young's modulus, E	207 GPa
Radius of journal, R_j	9.9 mm	Poisson ratio, σ	0.3
Radial clearance, c_r	0.1 mm	Mass of journal	0.05 kg
Coefficient of restitution, c_e	0.9	Moment of inertia of journal	2.45×10^{-6} kg m^2

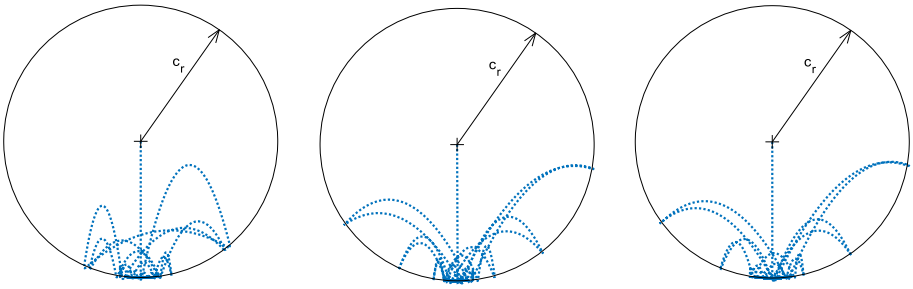

(a) Brown and McPhee model (b) LuGre model (c) LuGre model modified

Fig. 11 Comparison of journal eccentricity for different friction models

eccentricity varies within the clearance circle); (ii) impact (if the eccentricity line rebounds on the clearance circle); and (iii) continuous contact (when the eccentricity line overlaps the clearance circle during a given time). It can be observed that the friction models considered present significantly different motion. On the one hand, the Brown and McPhee model has some impacts on the lower side of the bearing and tends to stabilize the motion, while the LuGre and LuGre modified models lead to impacts in a wider area of the bearing. Another important quantity to discuss is the normal force and its relationship with friction force. Figure 12 (left) depicts the variation of the normal contact force. It can be observed that due to initial impacts, the normal load can be around 100 times higher than the static equilibrium load. Moreover, this variation during the impacts is highly abrupt which affects the capacity of the LuGre model to correctly capture frictional behavior. As can be seen in Fig. 12 (right), the ratio of friction and normal forces only shows acceptable values, i.e., not exceeding the static coefficient of friction, for the Brown and McPhee friction model. For the LuGre model, this value is largely surpassed, even after the initial impacts (see detailed plot in Fig. 12d). Although the modified version of LuGre model presents a lower ratio between friction and normal force, it still provides an inadmissible value, which does not make the simulation results as reliable. As it was mentioned in the previous section, the normal force variation is not the only issue associated with the LuGre model. Hence, the damping term is not scaled for a certain problem, therefore, it may dominate the friction magnitude.

Finally, the mechanical energy variation of the system was analyzed, as it is represented in Fig. 13. The Brown and McPhee model depicts a slightly faster dissipation of the mechanical energy of the journal. However, all friction models show that the damping in the impacts and the energy dissipated through friction lead to the continuous energy loss, which makes the journal to almost stop its motion after around 0.2 s. The LuGre model presents more instability on energetic evolution of the system.

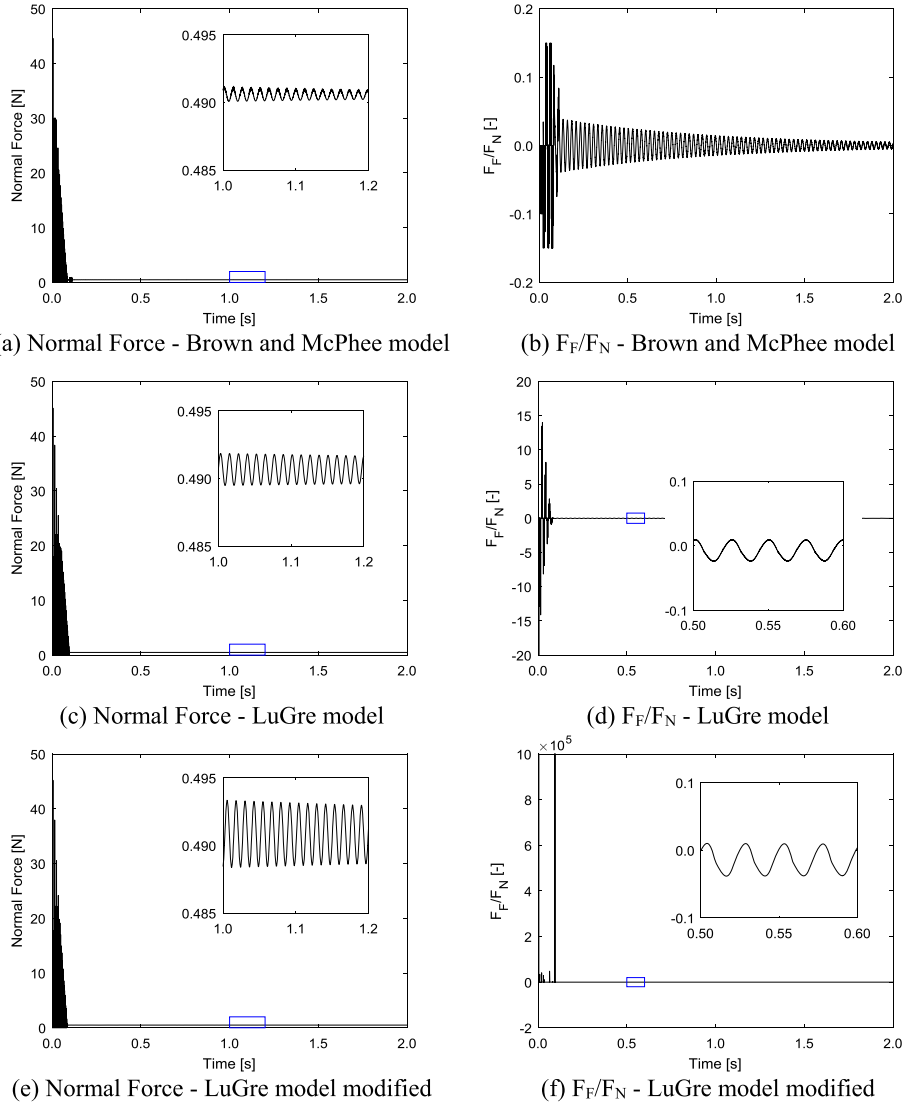

(a) Normal Force - Brown and McPhee model

(b) F_F/F_N - Brown and McPhee model

(c) Normal Force - LuGre model

(d) F_F/F_N - LuGre model

(e) Normal Force - LuGre model modified

(f) F_F/F_N - LuGre model modified

Fig. 12 Comparison of normal force and ratio between both friction and normal forces for different friction models

6 Concluding remarks

The modeling of frictional effects in the context of multibody dynamics formulation has been discussed in this study. In the sequel of this process, several issues related with implementation and parameters estimation of various friction models have been examined. Some of the most popular friction force models were revisited, and their main advantages and limitations were identified, as well as their capability to capture different frictional phenomena. The static models present easiness of implementation point of view, while in general, the dynamic models can describe more frictional characteristics due to extra state variable

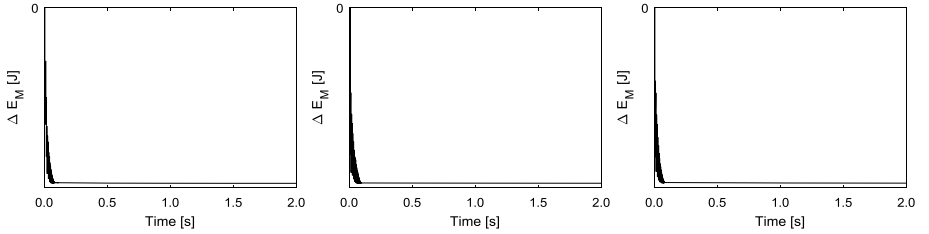

(a) Brown and McPhee model (b) LuGre model (c) LuGre model modified

Fig. 13 Comparison of mechanical energy variation for different friction models

and more parameters. Then, the inclusion of frictional forces in the equations of motion of a constrained multibody system has been discussed, wherein different approaches were considered depending on the type of problem to be solved.

Two examples of application were presented to examine the influence of the different friction force models on the dynamic response of a multibody system where rolling motion may occur. In the first example, the dynamic behavior of a roller–crank mechanism was examined, where friction force was considered in the contact between the roller and the ground. The second example considered the impact motion of a simple journal–bearing system. Thus, it is possible to compare how the different models behave with continuous and impact motion, respectively. In the first example, the static models with discontinuity at zero velocity and models without static friction were not able to capture the correct motion during the pure rolling phase, where the surfaces were sticking together. Moreover, the normal load variations showed to have an undesirable effect on the frictional force obtained through dynamic models. In the second example, the variations of normal load were more abrupt due to the impact motion between the journal and bearing. These variations of normal force completely influence the friction force obtained by a dynamic friction model, namely the LuGre, in which the results may not be reliable.

Overall, a static friction model which accounts for the static friction and avoids force discontinuity, such as the Brown and McPhee, is most of the time a suitable choice for modeling friction since it captures the most relevant friction characteristics. It requires a small number of parameters and does not increase significantly the computational time. In turn, the use of a dynamic model, such as LuGre model, helps to capture some more detailed phenomena, namely frictional lag or pre-sliding displacement. However, it was clearly shown that this model may not be able to provide reliable results for the examined application examples, even considering modified approaches. The need of developing an alternative methodology for accurately model friction forces with a dynamic model without increasing its complexity can be highlighted as a future direction of research.

Acknowledgements The first author expresses his gratitude to the Portuguese Foundation for Science and Technology through the PhD grant (PD/BD/114154/2016), MIT Portugal Program. This work has been supported by the Portuguese Foundation for Science and Technology with the reference project UID/EEA/04436/2013, by FEDER funds through the COMPETE 2020—*Programa Operacional Competitividade e Internacionalização* (POCI) with the reference project POCI-01-0145-FEDER-006941.

References

1. Johnson, K.L.: Contact Mechanics. Cambridge University Press, Cambridge (1985). ISBN 0521347963
2. Kalker, J.J.: Three-Dimensional Elastic Bodies in Rolling Contact. Springer, Netherlands (1990). ISBN 9789048140664
3. Popov, V.: Contact Mechanics and Friction: Physical Principles and Applications. Springer, Berlin (2017). ISBN 978-3-662-53080-1
4. Hertz, H.: Über die Berührung fester elastischer Körper. J. Reine Angew. Math. **92**, 156–171 (1881)
5. Coulomb, C.A.: Théorie des machines simples, en ayant égard au frottement de leurs parties, et à la roideur des cordages. Mémoire de Mathématique et de Physique, Paris (1785)
6. Flamant, A.: Sur la répartition des pressions dans un solide rectangulaire chargé transversalement. C. R. Acad. Sci. Paris **114**, 1465–1468 (1892)
7. Timoshenko, S.: Theory of Elasticity. McGraw-Hill, New York (1951)
8. Hunter, S.C.: The rolling contact of a rigid cylinder with a viscoelastic half-space. J. Appl. Mech. **28**(4), 611–617 (1961)
9. Bhargava, V., Hahn, G., Rubin, C.A.: An elastic-plastic finite element model of rolling contact, part 2: analysis of repeated contacts. J. Appl. Mech. **52**(1), 75–82 (1985)
10. Hamrock, B.J., Dowson, D.: Ball Bearing Lubrication: The Elastohydrodynamics of Elliptical Contacts. Wiley-Interscience, New York (1981)
11. Bower, A.F., Johnson, K.L.: The influence of strain hardening on cumulative plastic deformation in rolling and sliding line contact. J. Mech. Phys. Solids **3784**, 471–493 (1989)
12. Ringsberg, J.W.: Life prediction of rolling contact fatigue crack initiation. Int. J. Fatigue **23**(7), 575–586 (2001)
13. Raje, N., Sadeghi, F., Rateick, R.: A statistical damage mechanics model for subsurface initiated spalling in rolling contacts. J. Tribol. **130**(4), 042201 (2008), 11 pp.
14. Pöschel, T., Schwager, T., Brilliantov, N.V.: Rolling friction of a hard cylinder on a viscous plane. Eur. Phys. J. B **10**(1), 169–174 (1999)
15. Stolarski, T.A., Tobe, S.: Rolling Friction. Tribology in Practice Series. Wiley, Chichester (2001)
16. Cherepanov, G.P.: Theory of rolling: solution of the Coulomb problem. J. Appl. Mech. Tech. Phys. **55**(1), 182–189 (2014)
17. Johnson, K.L., Kendall, K., Roberts, A.D.: Surface energy and the contact of elastic solids. Proc. R. Soc. A **324**, 301–313 (1971)
18. Derjaguin, B.V., Muller, V.M., Toporov, Y.P.: Effect of contact deformations on the adhesion of particles. J. Colloid Interface Sci. **53**(2), 314–326 (1975)
19. Armstrong-Hélouvry, B., Dupont, P., Canudas de Wit, C.: A survey of models, analysis tools and compensation methods for the control of machines with friction. Automatica **30**, 1083–1138 (1994)
20. Olsson, H., Åström, K.J., Canudas de Wit, C., Gäfvert, M., Lischinsky, P.: Friction models and friction compensation. Eur. J. Control **4**, 176–195 (1998)
21. Awrejcewicz, J., Olejnik, P.: Analysis of dynamic systems with various friction laws. Appl. Mech. Rev. **58**(6), 389–411 (2005)
22. Pennestrì, E., Rossi, V., Salvini, P., Valentini, P.P.: Review and comparison of dry friction force models. Nonlinear Dyn. **83**(4), 1785–1801 (2016)
23. Marques, F., Flores, P., Claro, J.C.P., Lankarani, H.M.: A survey and comparison of several friction force models for dynamic analysis of multibody mechanical systems. Nonlinear Dyn. **86**(3), 1407–1443 (2016)
24. Bowden, F.P., Tabor, D.: Friction and Lubrication of Solids. Oxford Univ. Press, London (1950)
25. Rubenstein, C.: A general theory of the surface friction of solids. Proc. Phys. Soc. B **69**, 921 (1956)
26. Archard, J.F.: Elastic deformation and the laws of friction. Proc. R. Soc. A **243**(1233), 190–205 (1957)
27. Suh, N.P., Sin, H.C.: The genesis of friction. Wear **69**(1), 91–114 (1981)
28. Curnier, A.: A theory of friction. Int. J. Solids Struct. **20**(7), 637–647 (1984)
29. Zhang, J., Moslehy, F.A., Rice, S.L.: A model for friction in quasi-steady-state sliding. Wear **149**(1–2), 1–25 (1991)
30. Straffelini, G.: A simplified approach to the adhesive theory of friction. Wear **249**(1–2), 78–84 (2001)
31. Berger, E.J.: Friction modeling for dynamic system simulation. Appl. Mech. Rev. **55**(6), 535–577 (2002)
32. Martins, J.A., Faria, L.O., Guimarães, J.: Dynamic surface solutions in linear elasticity and viscoelasticity with frictional boundary conditions. J. Vib. Acoust. **117**, 445–451 (1995)
33. Bigoni, D.: Nonlinear Solid Mechanics: Bifurcation Theory and Material Instability. Cambridge University Press, Cambridge (2012). ISBN 978-1107025417
34. Rice, J.R., Ruina, A.L.: Stability of steady frictional slipping. J. Appl. Mech. **50**(2), 343–349 (1983)
35. Flint, J., Hultén, J.: Lining-deformation-induced modal coupling as squeal generator in a distributed parameter disk brake model. J. Sound Vib. **254**, 1–21 (2002)

36. Rabinowicz, E.: Stick and slip. Sci. Am. **194**, 109–118 (1956)
37. Awrejcewicz, J., Olejnik, P.: Occurrence of stick-slip phenomenon. J. Theor. Appl. Mech. **35**, 33–40 (2007)
38. Berger, E.J., Mackin, T.J.: On the walking stick-slip problem. Tribol. Int. **75**, 51–60 (2014)
39. Flores, P., Ambrosio, J., Claro, J.C.P.: Dynamic analysis for planar multibody mechanical systems with lubricated joints. Multibody Syst. Dyn. **12**, 47–74 (2004)
40. Stefanelli, R., Valentini, P.P., Vita, L.: Modelling hydrodynamic journal bearing in 3D multibody systems. In: Proceedings of ASME-IDETC/CIE 2005, Long Beach, California, USA, Sept. 24–28 (2005)
41. Feng, X., Bai, W.: Hydrodynamic analysis of marine multibody systems by a nonlinear coupled model. J. Fluids Struct. **70**, 72–101 (2017)
42. Wu, X.D., Zuo, S.G., Lei, L., Yang, X.W., Li, Y.: Parameter identification for a LuGre model based on steady-state tire conditions. Int. J. Automot. Technol. **12**(5), 671–677 (2011)
43. Yoon, J.Y., Trumper, D.L.: Friction modeling, identification, and compensation based on friction hysteresis and Dahl resonance. Mechatronics **24**, 734–741 (2014)
44. Piatkowski, T.: Dahl and LuGre dynamic friction models—the analysis of selected properties. Mech. Mach. Theory **73**, 91–100 (2014)
45. Sun, Y.-H., Chen, T., Wu, C.Q., Shafai, C.: A comprehensive experimental setup for identification of friction model parameters. Mech. Mach. Theory **100**, 338–357 (2016)
46. Piatkowski, T., Wolski, M.: Analysis of selected friction properties with the Froude pendulum as an example. Mech. Mach. Theory **119**, 37–50 (2018)
47. Canudas de Wit, C., Olsson, H., Åström, K.J., Lischinsky, P.: A new model for control of systems with friction. IEEE Trans. Autom. Control **40**, 419–425 (1995)
48. Do, N.B., Ferri, A.A., Bauchau, O.A.: Efficient simulation of a dynamic system with LuGre friction. J. Comput. Nonlinear Dyn. **2**, 281–289 (2007)
49. Saha, A., Wahi, P., Wiercigroch, M., Stefański, A.: A modified LuGre friction model for an accurate prediction of friction force in the pure sliding regime. Int. J. Non-Linear Mech. **80**, 122–131 (2016)
50. Wojtyra, M.: Comparison of two versions of the LuGre model under conditions of varying normal force. In: ECCOMAS Thematic Conference on Multibody Dynamics, Prague, Czech Republic, (2017), 10 pp.
51. Halme, J., Andersson, P.: Rolling contact fatigue and wear fundamentals for rolling bearing diagnostics. Proc. Inst. Mech. Eng., Part J J. Eng. Tribol. **224**, 377–393 (2009)
52. Threlfall, D.C.: The inclusion of Coulomb friction in mechanisms programs with particular reference to DRAM au programme DRAM. Mech. Mach. Theory **13**, 475–483 (1978)
53. Ambrósio, J.A.C.: Impact of rigid and flexible multibody systems: deformation description and contact model. Virtual Nonlinear Multibody Syst. **103**, 57–81 (2003)
54. Andersson, S., Söderberg, A., Björklund, S.: Friction models for sliding dry, boundary and mixed lubricated contacts. Tribol. Int. **40**, 580–587 (2007)
55. Tustin, A.: The effects of backlash and of speed-dependent friction on the stability of closed-cycle control systems. J. Inst. Electr. Eng. **94**, 143–151 (1947)
56. Hess, D.P., Soom, A.: Friction at a lubricated line contact operating at oscillating sliding velocities. J. Tribol. **112**, 147–152 (1990)
57. Popp, K., Stelter, P.: Nonlinear oscillations of structures induced by dry friction. In: Nonlinear Dynamics in Engineering Systems, pp. 233–240 (1990)
58. Armstrong-Hélouvry, B.: Control of Machines with Friction. Kluwer Academic Publishers, Norwell (1991)
59. Makkar, C., Dixon, W.E., Sawyer, W.G., Hu, G.: A new continuously differentiable friction model for control systems design. In: Proceedings of the 2005 IEEE/ASME, International Conference on Advanced Intelligent Mechatronics, pp. 600–605 (2005)
60. Specker, T., Buchholz, M., Dietmayer, K.: A new approach of dynamic friction modelling for simulation and observation. In: 19th World Congress of the International Federation of Automatic Control, Cape Town, South Africa, Aug. 24–29, pp. 4523–4528 (2014)
61. Brown, P., McPhee, J.: A continuous velocity-based friction model for dynamics and control with physically meaningful parameters. J. Comput. Nonlinear Dyn. **11**(5), 054502 (2016)
62. Bowden, F.P., Leben, L.: The nature of sliding and the analysis of friction. Proc. R. Soc. Lond. Ser. A, Math. Phys. Sci. **169**, 371–391 (1939)
63. Johannes, V.I., Green, M.A., Brockley, C.A.: The role of the rate of application of the tangential force in determining the static friction coefficient. Wear **24**, 381–385 (1973)
64. Dahl, P.R.: A solid friction model. Technical report. The Aerospace Corporation, El Segundo, California (1968)
65. Dahl, P.R.: Solid friction damping in mechanical vibrations. AIAA J. **14**, 1675–1682 (1976)
66. Lampaert, V., Al-Bender, F., Swevers, J.: A generalized Maxwell-slip friction model appropriate for control purposes. In: Proceedings of IEEE International Conference on Physics and Control, St. Petersburg, Russia, pp. 1170–1178 (2003)

67. Al-Bender, F., Lampaert, V., Swevers, J.: The generalized Maxwell-slip model: a novel model for friction simulation and compensation. IEEE Trans. Autom. Control **50**, 1883–1887 (2005)
68. Nikravesh, P.E.: Computer Aided Analysis of Mechanical Systems. Prentice Hall, Englewood Cliffs (1988)
69. Marques, F., Souto, A.P., Flores, P.: On the constraints violation in forward dynamics of multibody systems. Multibody Syst. Dyn. **39**(4), 385–419 (2017)
70. Baumgarte, J.: Stabilization of constraints and integrals of motion in dynamical systems. Comput. Methods Appl. Mech. Eng. **1**, 1–16 (1972)
71. Flores, P., Machado, M., Seabra, E., Silva, M.T.: A parametric study on the Baumgarte stabilization method for forward dynamics of constrained multibody systems. J. Comput. Nonlinear Dyn. **6**(1), 0110191 (2011)
72. Haug, E.J., Wu, S.C., Yang, S.M.: Dynamics of mechanical systems with Coulomb friction, stiction, impact, and constraints addition, deletion—I theory. Mech. Mach. Theory **21**(5), 401–406 (1986)
73. Wu, S.C., Yang, S.M., Haug, E.J.: Dynamics of mechanical systems with Coulomb friction, stiction, impact, and constraints addition, deletion—II planar systems. Mech. Mach. Theory **21**(5), 407–416 (1986)
74. Wu, S.C., Yang, S.M., Haug, E.J.: Dynamics of mechanical systems with Coulomb friction, stiction, impact, and constraints addition, deletion—II spatial systems. Mech. Mach. Theory **21**(5), 417–425 (1986)
75. Frączek, J., Wojtyra, M.: On the unique solvability of a direct dynamics problem for mechanisms with redundant constraints and Coulomb friction in joints. Mech. Mach. Theory **46**(3), 312–334 (2011)
76. Haug, E.J.: Simulation of friction and stiction in multibody dynamics model problems. Mech. Based Des. Struct. Mach. **46**(3), 296–317 (2018)
77. Wojtyra, M.: Modeling of static friction in closed-loop kinematic chains—uniqueness and parametric sensitivity problems. Multibody Syst. Dyn. **39**(4), 337–361 (2017)
78. Harlecki, A., Urbaś, A.: Modelling friction in the dynamics analysis of selected one-DOF spatial linkage mechanisms. Meccanica **52**, 403–420 (2017)
79. Pennestrì, E., Valentini, P.P., Vita, L.: Multibody dynamics simulation of planar linkages with Dahl friction. Multibody Syst. Dyn. **17**(4), 321–347 (2007)
80. Wojtyra, M.: On some problems with modeling of Coulomb friction in self-locking mechanisms. J. Comput. Nonlinear Dyn. **11**(1), 011008 (2016)
81. Gholami, F., Nasri, M., Kövecses, J., Teichmann, M.: A linear complementarity formulation for contact problems with regularized friction. Mech. Mach. Theory **105**, 568–582 (2016)
82. Flores, P., Ambrósio, J.: Revolute joints with clearance in multibody systems. Comput. Struct. **82**(17–19), 1359–1369 (2004)
83. Lankarani, H.M., Nikravesh, P.E.: A contact force model with hysteresis damping for impact analysis of multibody systems. J. Mech. Des. **112**(3), 369–376 (1990)
84. Tian, Q., Flores, P., Lankarani, H.M.: A comprehensive survey of the analytical, numerical and experimental methodologies for dynamics of multibody mechanical systems with clearance or imperfect joints. Mech. Mach. Theory **122**, 1–57 (2018)
85. ISO 286-1:2010 (en). Geometrical product specifications (GPS)—ISO code system for tolerances on linear sizes—part 1: basis of tolerances, deviations and fits